J.Natn.Sci.Foundation Sri Lanka 2024 52 (1): 35 - 44
DOI: http://dx.doi.org/10.4038/jnsfsr.v52i1.11360

RESEARCH ARTICLE

Opthalmic Genetics

Prevalence and *in silico* analysis of p.D658G variant of *WDR36* gene in patients affected with primary open angle glaucoma from Punjab Pakistan

Khazeema Yousaf [1], Zernish Shabbir[1], Rasheeda Bashir[1*], Syed Mohsin Raza[2], Saiqa Ilyas[1] and Rukhama Haq[1]

[1] *Department of Biotechnology, Lahore College for Women University, Lahore, Pakistan.*
[2] *Institute of Biomedical and Health Sciences, University of Health Sciences, Lahore, Pakistan.*

Submitted: 26 July 2022; Revised: 11 July 2023; Accepted: 28 July 2023

Abstract: The aim of the present study was to check the frequency of genetic variants in exons 8, 11, 13, and 17 of the *WDR36* gene among primary open angle glaucoma (POAG) patients from Punjab, Pakistan, and to perform the *in silico* analysis of identified variants on protein function. Ninety-two individuals affected with primary open angle glaucoma were enrolled for this study. The clinical investigation involved the examination of the optic nerve head, visual field loss and elevated intraocular pressure (IOP). Selected exons (8, 11, 13, and 17) of the *WDR36* gene was screened by Sanger sequencing. Sequencing results revealed a previously reported missense mutation p.D658G in exon 17 in two out of ninety-two POAG patients, while no mutation has been identified in the exons 8, 11, and 13. To predict the structural and functional effect of the p.D658G variant, SIFT, Polyphen-2, PROVEAN, mutation taster, I-mutant 3.0, and MuPRO were used. The MODELLER-CABS based hybrid approach was used for protein structure modelling. *In silico* analysis predicted the p.D658G variant to be deleterious, and it may affect the stability of protein and protein-protein interaction. The findings of this study suggested that the genetic variant p.D658G of the *WDR36* gene is a rare genetic cause of POAG in Pakistani patients. The *in silico* tools predicted the variant p.D658G to be deleterious; however the modelled normal and mutant structure showed no effect on protein structure and function. To further confirm the pathogenic effect of this SNP, *in vivo* experiments, X-ray Crystallography of the WDR36 protein and population-based studies are needed.

Keywords: Intra ocular pressure, latent transforming growth factor-beta Protein 2, primary open angle glaucoma, WD repeat domain 36.

INTRODUCTION

Primary open angle glaucoma (POAG) is a heterogeneous group of optic neuropathies that lead to optic nerve damage and permanent vision loss (Mbacham *et al*., 2020). POAG is the most prevalent form of glaucoma particularly in Asia. A study from Pakistan reported that the prevalence of POAG is 40.3% among the 3021 glaucoma patients enrolled while the overall glaucoma prevalence was 8.5% (Akhtar *et al*., 2010). Clinical symptoms of POAG includes ocular hypertension, elevated intraocular pressure (> 22 mmHg) called high tension glaucoma (HTG) (Bui *et al*., 2005) and low-tension glaucoma (LTG) or normal tension glaucoma (NTG) with IOP < 22 mmHg (Miyazawa *et al*., 2007). Individuals having age more than 40 years showed greater susceptibility to glaucoma; also, men are more prone to POAG than females (Tham *et al*., 2014).

The precise molecular basis of POAG is still not well known. It is a genetically heterogeneous disorder caused

* Corresponding author (rashidasbs@yahoo.com; https://orcid.org/0000-0003-1270-3742)

by the involvement of multiple genes and environmental factors. Till now, at least 14 loci from Glaucoma (GLC)1A to GLC1N have been linked to POAG (Monemi *et al*., 2005) and the following genes, *viz.*, Myocilin (*MYOC*), Optineurin (*OPTN*) (Rezaie *et al*., 2002), WD repeat domain 36 (*WD40-Repeat36*) (Monemi *et al*., 2005), neurotrophin *4 (NTF4)* (Rezaie *et al*., 2002), optic atrophy *1 (OPA1)* (Monemi *et al*., 2005), cytochrome P450 family 1, subfamily B *(CYP1B1)* (Kaur *et al*., 2011), and latent transforming beta binding protein 2 *(LTBP2)* are associated with POAG (Su *et al*., 2017). The gene *WDR36* is known as a gene, out of many other genes, which can cause POAG and is recognized as a cause of POAG pathogenesis (Youngblood *et al*., 2019). WD repeat domain 36 is a class of a nucleolar protein encoded by WDR36 and is involved in the maturation of 18s rRNA. *WDR36* is a member of the *WD40* repeat protein family, and helps in T- cell activation (Rezaie *et al*., 2002). The T-cell mediated response participates in optic nerve degeneration (Padgett & Glaser 2003).

POAG caused by mutations at in *WDR36* gene alone contribute 5% of all reported cases (Fuse 2010). The worldwide prevalence of *WDR36* gene mutations in patients affected with POAG is 1.6-1.7% (Mbacham *et al*., 2020). The WD repeat domain 36 is a class of nucleolar protein encoded by WDR36 and is involved in the maturation of 18s rRNA. The exact role of *WDR36* gene mutations in causing POAG is controversial in previously published data (Weisschuh *et al*., 2007). In a study from German population, it is reported that *WDR36* gene variants are rare causes of NTG (Weisschuh *et al*., 2007). It is also suggested in another study by Pasutto *et al.* (2008) that WDR36 plays a minor contributing role in causing POAG in same population, whereas another investigation suggested that WDR36 sequence variants can lead to diseased phenotype in polygenic forms of glaucoma (Footz *et al*., 2009). Four alterations (N355S, D658G, R529Q, and A449T) were identified between 17 distinct POAG subjects (Monemi *et al*., 2005). Different mutation patterns in p.D658G of *WDR36* of about 1-2% were reported in a German cohort, 1.7% in St. Petersburg, Russia (Motushchuk *et al*., 2009), and 1% in Italy (Frezzotti *et al*., 2011).

The genetics of POAG due to *WDR36* gene has not been explored in Pakistan, so the aim of this study was to check the pathogenic variants in selected exon 8, 11, 13, and 17 in the *WDR36* gene among POAG patients of Punjab, Pakistan and to analyze the damaging effect of identified variants on the function of the WDR36 protein by using various *in silico* tools. The *WDR36* Protein structure was modeled to analyze the deleterious effect of variant p.D658G on protein 3-D structure.

MATERIALS AND METHODS

The study was carried out at the Department of Biotechnology, Lahore College for Women University. Approval was granted from the Institutional Review Board (IRB), Lahore. Ninety-two POAG affected patients were enrolled after diagnosis by ophthalmologists from the Mughal Eye Hospital, Lahore. One hundred (100) controls belonging to the same ethnic background were also enrolled. Written consent was obtained from all individuals. All clinical parameters were recorded, *i.e.*, age of onset of disease, family history, visual acuity, cup to disc ratio (C/D) and increased intraocular pressure. An intravenous blood sample (5 cc) was taken from each individual in EDTA coated tubes (BD, USA) and stored at 4 °C.

Molecular genetic analysis

DNA was extracted using sucrose lysis and the method of salt precipitation. PCR was performed for the amplification of exons 8, 11, 13, and 17 (details provided in supplementary Table 1). The primers were designed using Primer 3 software (http://biotools.umassmed.edu/bioapps/primer3_www.cgi) (supplementary Table 1). The specific set of primers was prepared with a final volume of 25 µL, with 0.15 - 0.25 units of *Thermus aquaticus* DNA (TaqDNA) polymerase (MBI Fermentas, Vilnius, Lithuania) having a volume of 2.5 µL of Taq buffer, 2 mM $MgCl_2$, 0.2 mM DNTPs, 0.24 µL forward primer and 0.24 µL reverse primer (with 0.24 µM concentration of each primer), and 50 ng genomic DNA. Initial denaturation of DNA was performed at 94 ºC for 4 min followed by 36 cycles of denaturation at 95 ºC for 30 s, and annealing at 55 ºC for exon 11 and 17, and 56 ºC and 57 ºC for exon 8 and 13, respectively, for 30 s. The initial extension was at 75 ºC for 1 min and final extension was performed at 75 ºC for 5 min. PCR products were purified by a gene cleaning column (Gel Extraction Kit Thermo Scientific GeneJet) and were sequenced by direct sequencing with Big Dye Terminator® (V 3.1) Cycle Sequencing Kit (Applied Biosystems, Foster City, CA). The samples were resolved on an ABI 3730 capillary machine.

In silico analysis

Once the sequencing files were acquired, they were exported to SEQMAN, a software tool in the Lasergene suite from DNASTAR. Normal sequences of *WDR36* gene exons 8, 11, 13, and 17 were obtained from the UCSC genome browser website (http://genome.ucsc.edu/) and were used for analyzing the trace files. ClustalOmega was used for multiple alignment of WDR protein sequences

of different species to check the conservation domain on D658 residue (Figure 1E). To check the damaging effect on protein structure Polyphen, Mutation taster and PROVEAN were applied. The PolyPhen server provides a damaging scale ranging from 0.00-1, wherein a score near to 1 has been regarded as potentially damaging. The PROVEAN tool predicts whether an amino acid variation has a damaging impact on the biological functionality of a protein. To check the damaging effects of mutation on the stability of the protein, I-Mutant2.0 and MuPRO tools were used. The I-Mutant server predicts the effect of mutations on the stability of a protein.

Modelling the complete WDR36 protein

Currently, there is no crystal structure available for the WDR36 protein. Thus, an NCBI BLASTp (PSI-BLAST) (Altschul *et al*., 1997) search was performed, using PDB as the search source, to find closely related protein structures. Among the results, the top 3 structures (Table 3) were chosen for homology modelling. For the modelling of the WDR36 protein, the MODELLER-CABS hybrid approach was adopted (Van Koolwijk *et al*., 2007; Jamroz & Kolinski, 2010). The part of the protein which was covered by templates was modelled by homology modelling using MODELLER v9.24 (Eswar *et al*., 2006; Webb & Sali., 2016). MODELLER utilizes python scripts, to perform various steps of homology modelling. The basic steps involved were alignment of the structures of the three templates, their alignment with query sequence, model building based on multiple templates-query sequence alignment, followed by model evaluation by DOPE (discrete optimized protein energy) score. The top 10 resulting models with the lowest DOPE score were selected for the modelling of the N- and C-terminal regions for which templates provided no coverage. The chosen top 10 models were submitted to the online CABS-fold server (Blaszczyk *et al*., 2013) (http://biocomp.chem.uw.edu.pl/CABSfold/index.php) as templates along with the WDR36 protein sequence, to model the N- and C-terminal part of protein. The structures provided by CABS-Fold server were in the form of clusters (models) ranked according to the cluster densities. The cluster with highest density was selected as the predicted model. The loops of this model were further refined again by MODELLER v9.24, and the resulting model with the lowest DOPE score was saved as the WDR36 native model.

Mapping of p.D658G variant on the structure of the protein

The best structure chosen after the loop refinement was used as native protein. The mutated model was generated by using the Swiss-PDBViewer ver. 4.10, which allows browsing through a rotamer library to change amino acids (Guex *et al*., 1997). In order to substitute native amino acid with mutated one, the mutation tool was used. The mutation tool allows the placement of the best rotamer for the new amino acid. The mutated structure was saved in the .pdb format. The energy minimization of both the native and mutant structure was also performed by the GROMOS96 implementation of Swiss-PDBViewer by the conjugate gradient method.

Calculation of RMSD value of modelled protein

For the calculation of root-mean-square deviation of the atomic positions in the mutated modeled protein, USCF Chimera ver 1.14 was used (Pettersen *et al*., 2004). The native and the mutated proteins were superposed, and the matchmaker command was applied to calculate the RMSD value between the native and mutated protein structure. The extent of structural deviation calculated based on RMSD value shows that the higher the RMSD value, the higher will be the deviation of structure and related function of the protein (Coutsias *et al*., 2004).

Validation of native and mutant models

The Ramachandran plot calculates the dihedral angles of the amino acid residues. These phi and psi dihedral angles help in calculating the energetically allowed resides, helping in understanding the structural and functional properties of protein structure. Both the native and mutant protein structures were evaluated by the online tool PROCHECK (https://servicesn.mbi.ucla.edu/PROCHECK/) (Laskowski *et al*., 1993).

RESULTS AND DISCUSSION

The study was designed to check the contribution of the selected exons (8, 11, 13, and 17) of the *WDR36* gene among POAG patients from Punjab. The age range of patients involved in our study was 41-65 years (mean, 52.7 ± 9.8). The average IOP was 23.5 ± 8.10. Table 1 represents the baseline characteristics of the patients. Clinical features of POAG patients showed watery eyes,

enlarged globe and hazy cornea. In patients (POAG II & III) the IOP ranged from 40 to 50 mmHg. The P-value showed a significant difference between control and diseased individuals' IOP and C/D ratio (Table 1). It was also observed in POAG patients that IOP of the right eye was greater than that of the left eye, and the percentage of men affected with POAG was greater than that of women (Figures 1 A and 1 B).

Table 1: Clinical parameters of POAG and control groups

Parameters	Status	POAG	Control	P Value	
Sex	Male	56	50		
	Female	36	50		
Age	Mean ± SD	52.78 ± 9.8	65.9 ± 11.6		
	Range	41 - 65	41 - 93		
Max. IOP	Mean ± SD	23.6 ± 8.1	15.0 ± 2.7	Left eye	Right eye
		8 – 60	8–21	0.0001*	0.01*
CD ratio	Male &	0.4 – 0.9	0.4	Left eye	Right eye
	Female			0.01*	0.01*

* indicates the significant values

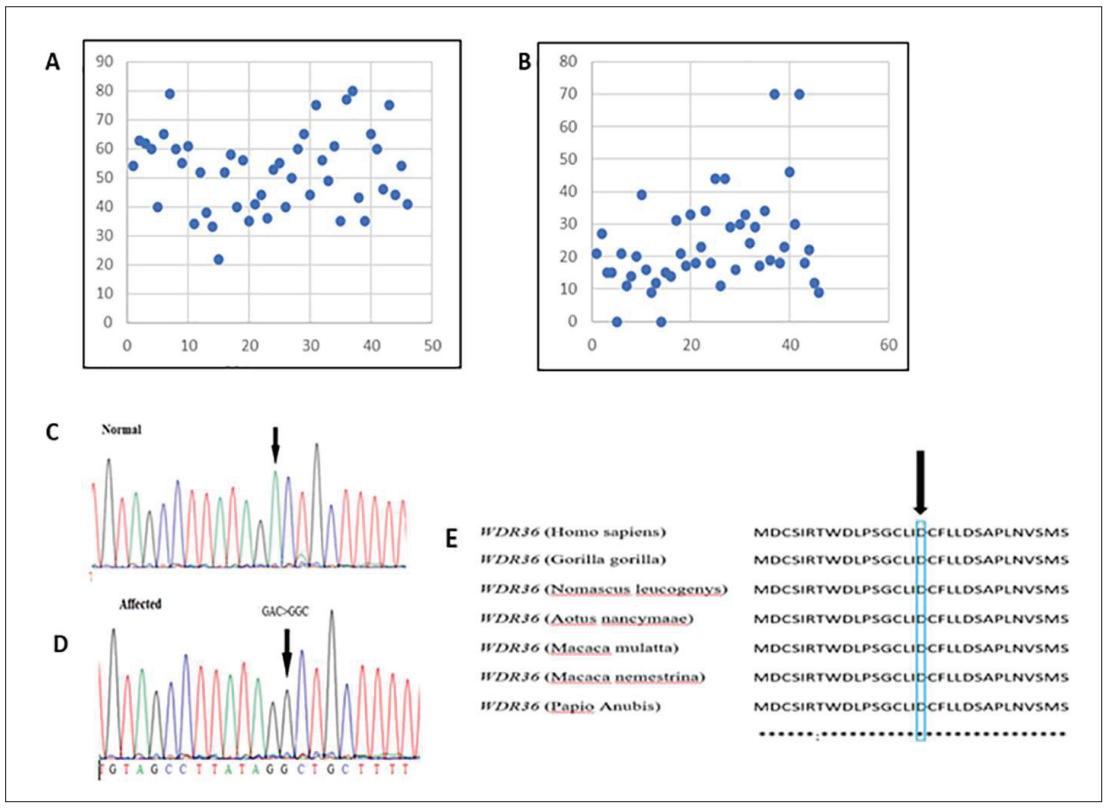

Figure 1: (A) IOP of right eye with respect to age among POAG patients; (B) IOP of left eye with respect to age among POAG patients; (C) Sequencing Chromatogram of Exon 17 of *WDR36* gene in normal and (D); POAG affected patient, the homozygous mutation c.1973A>G (p.D658G) is indicated by an arrow in the trace from normal individual; (E) ClustalOmega output, showing conservation of p.D658 residue among WDR protein from different species.

Sanger sequencing results of exon 8, 11, and 13 showed no mutation while mutation p.D658G has been identified in exon 17. PCR amplification of mutant variant p.D658G using a specific set of primers showed the amplicon size of 443 bp. The sequencing results revealed p.D658G mutation in 2 out of ninety-two POAG patients at exon 17. The mutational analysis of sequencing results was done by Edit Seq and Chromas revealed a previously reported homozygous missense mutation at nucleotide position 1973 where adenine was changed into guanine (c.1973A > G) in the affected individual (Figures 1C and 1 D).

Only 2 out of 92 patients showed mutation p.D658G thus giving the evidence that prevalence of this variant is low in Pakistani patients.

In silico analysis

The mutational effect of p.D658G using the Polyphen server was predicted to be 1 which showed the damaging effect. PROVEAN algorithm results showed that variant p.D658G is deleterious (Table 2). To check the damaging effects of the mutation on the stability of the protein, I-Mutant2.0 and MuPRO tools were used (Table 2). The I-Mutant server predicts the effect of mutations on the stability of protein. A score below 0 shows decreased stability of protein and a score higher than 0 indicates increased stability of protein. The results showed the DDG score of -3.57, indicating that the p.D658G substitution decreases the stability of the protein. MuPRo tool showed that the substitution reduces the stability of protein structure with a DDG score of -1.448.

Table 2: Summary of *in silico* tools used to predict the pathogenicity of p.D658G variant

Prediction tools	Prediction result	Severity score
Mutation taster	Disease causing	Deleterious
PolyPhen-2	Probably damaging	1
PROVEAN	Deleterious,	-6.409
	Decrease stability	-1.4485842
I-Mutant	Decrease stability	-3.57
SIFT	Intolerable	0.42

Modelling of the *WDR36* protein & model validations

Due to the absence of the PDB structure of the WDR36 protein, structure modelling was performed. The PSI-BLAST revealed that there were very few structures which shared similarity with our protein sequence, the highest being 33.99% similar (Table 3). The query coverage was also less between 67-89%. Keeping in view the low similarity templates and less coverage, a hybrid approach of modelling was adopted. MODELLER v9.24 was commanded to generate 30 more similar models using the 3 aligned templates 5JPQ, 4NSX, and 5TZS, and "WDR36-mult.ali" file. The tope 10 models were selected according to the widely practiced criteria for selecting top models, *i.e.*, DOPE score must be lowest and GA341 score highest. These models were presented to the CABS-Fold server to model the non-template region of the protein. The server provides various predicted structures, each representing a cluster of structures, while the structure with highest cluster density is chosen as the best structure. The CABS-Fold server provided 8 clusters and model 1 had the highest cluster density of 213, with an average cluster RMSD of 1.8. The loops for the model 1 were refined by using MODELLER to get the final structure WDR36.BL00030001.pdb, which was later renamed as WDR36 Native Protein (Figure 2A). The modelled structure was validated by PROCHECK. The analysis of WDR36 Native Protein by PROCHECK showed that 77.2% of the residues lie in the most favored regions, 18.7% were in additional allowed regions, 2.2% in possible generously allowed regions and 2.0% were in the disallowed regions (Figure 2B).

Table 3: Results of closely related protein search (NCBI PSI-BLAST)

Sr. No	PDB ID	Query cover	Per. identity	Chain
1	5JPQ	89%	31.88%	I
2	4NSX	68%	33.83%	A
3	5TZS	67%	33.99%	T

Mapping of p.D658G variant on the protein structure

The p.D658G variant was mapped onto the WDR36_ Native Protein by using the mutation tool in Swiss-PDBViewer. The resulting Structure was denoted as WDR36_Mutant Protein (Figure 3B). To mimic the *in vivo* folding settings and parameters, energy minimization of both the native and mutant structures was performed by Swiss-PDBViewer using conjugate gradients. The total post-energy minimization and energy of the WDR36_Native Protein was -42975.512 kJ/mol, while the WDR36_Mutant Protein showed a total energy of -42878.793 kJ/mol, *i.e.*, a 96.719 kJ/mol increase in the energy. This slight increase in the protein energy may slightly affect the protein stability and function.

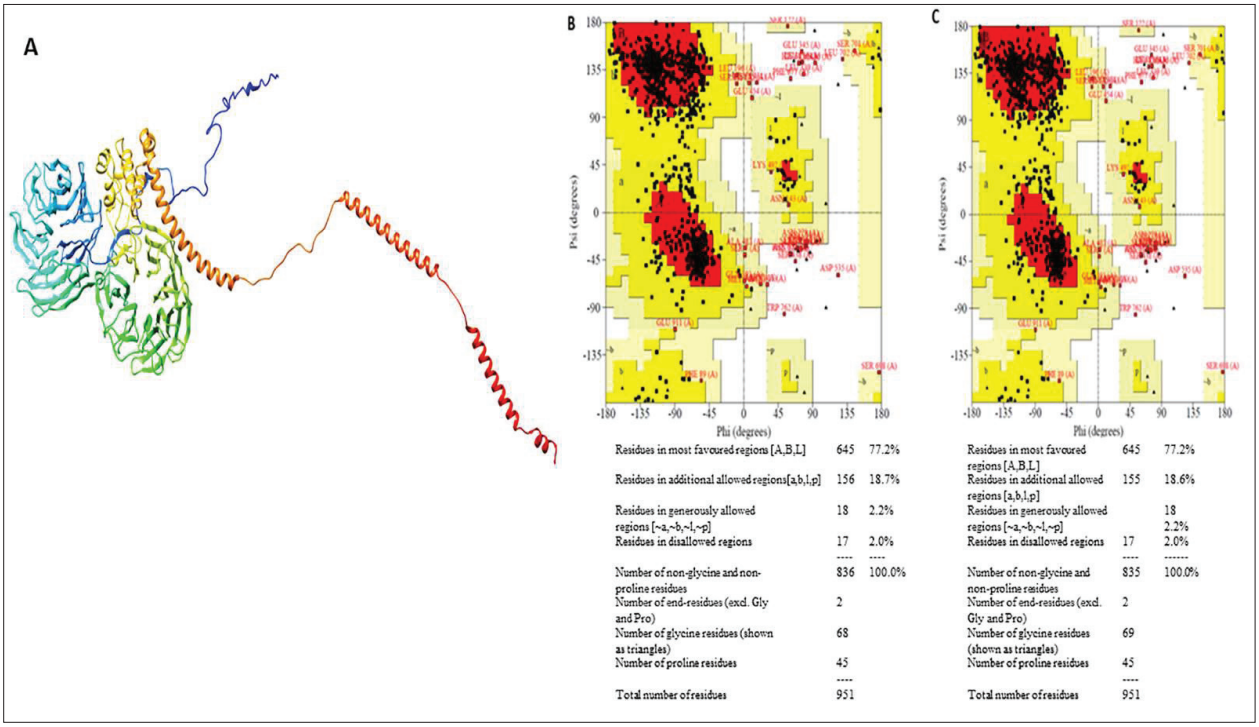

Figure 2: A) Representative model of WDR36 complete normal protein modelled by MODELLER-CABS hybrid approach B) Ramachandran plot of normal protein. C) Ramachandran plot of mutated protein.

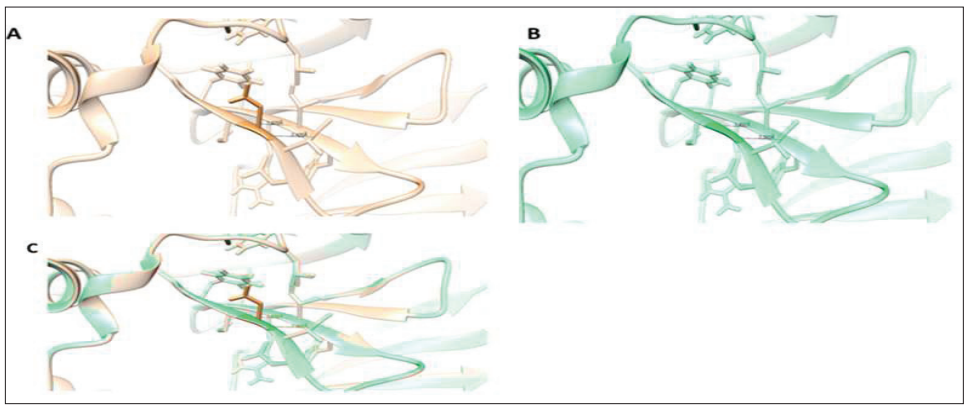

Figure 3: A) Representative model of WDR36 normal protein modelled by MODELLER-CABS hybrid approach; B) representative model of mutated protein generated by Swiss-PDBViewer.; C) superimposed structures of WDR36 normal protein and WDR36 mutant protein (RMSD = 0.004 Å). The images were modeled using USCF Chimera ver 1.14.

Calculating the RMSD value of the mutated protein

One of the important parameters for measuring the rate of deviation of normal and mutated protein structures is the method of root-mean-square deviation (RMSD). The mutant structure showed an RMSD value of 0.004 Å which shows that structure is not much deviated from the native structure. The hydrogen bond analysis shows that the number of hydrogen bonds are the same in both proteins on this position, with only some minor differences in the length of hydrogen bonds (Figures 3B and 3C).

Despite studies that have examined the involvement of the p.D658G variant of the *WDR36* gene in POAG patients in different population groups, no study has yet been reported from Pakistan to show the contributing role of the p.D658G mutation in Punjab POAG patients. Therefore, the present study was conducted to check the contribution of p.D658G of the *WDR36* gene in Punjab patients affected with POAG. The result of the study showed low prevalence of this mutant variant (c.1973A>G, p.D658G) in POAG patients in Punjab.

An analysis of published data revealed that this variant is associated with HTG cases (Miyazawa *et al*., 2007). In the current study, 2 patients carried the p.D658G variant. The POAG II patient was a 53 year old male, the IOP of his left eye was 45 mmHg and that of his right eye was 50 mmHg, with a 0.7/1 CD ratio. He had blurred vision with photophobia. The patient III was 55 years old; he had symptoms of blurred vision and photophobia. Clinical examination showed IOPs of 40 mmHg and 35 mmHg in the right and left eye, respectively. The CD ratio was 0.8/0.7 in the right and left eye, respectively.

From previous reports the p.D658G mutation has been attributed to about 1.94% of unrelated POAG patients in the US (Monemi *et al*., 2005). This mutation was previously found to be the more recurrent disease-causing allele in familial and non-familial cases (Monemi *et al*., 2005). The *WDR36* gene consists of four domains, which help in the T cell activation pathway, and any change in this gene is hypothesized to participate in optic nerve degeneration and a different form of glaucoma (Monemi *et al*., 2005). The p.D658G missense mutation is an exonic alteration and an important part of the *WDR36* gene, which results in the replacement of aspartic acid with lysine (acidic to basic amino acid) (Frezzotti *et al*., 2011).

The mutation p.D658G was also reported in the US as 1% (Monemi *et al*., 2005). However, further data on the involvement of this mutation in causing POAG was controversial. In the present study, the p.D658G mutation has been identified in two individuals out of 97. The mutation frequency of p.D658G in PAOG varied in different ethnic groups, with no mutation in Chinese and Japanese (Miyazawa *et al*., 2007; Huang *et al*., 2014), Australian and Russian populations (Motushchuk *et al*.,2009), but ranging from 1% to 3% in Spanish (Kaur *et al*., 2011), German, American (Monemi *et al*., 2005), and Italian (Frezzotti *et al*., 2011) populations. This data showed that, although it is a pathogenic mutation, its prevalence is low in different population, just as reported in the Pakistani population. These variations in mutational frequency may be due to different geographical regions, and environmental factors such as age, sex, race, and family history also contribute to causing POAG. Investigations of POAG patients from Australia and Germany (Monemi *et al*., 2005) suggest that variant p.D658G is a neutral variant, which signifies that variants of the *WDR36* gene may act as a causative factor in certain populations, or may act as a modifier gene for POAG in some other populations.

Residue D658 is a beta-sheet of the protein. D658 residue is located in separate G-beta WD40 repeats. The G proteins belong to a family of membrane-associated proteins and act as mediators in signal transduction induced by transmembrane receptors. The G-beta subunit is essential for anchoring to the membrane and recognition by the receptor. Structurally, the G-beta subunit comprises eight tandem repeats having 40 residues. Each residue contains a central Trp-Asp dipeptide bonding, thus named as WD40 repeats. Hence, mutations disturbing the structure of WD40 repeats may cause hindrance in the WDR36 interaction with other proteins (Tham *et al*., 2014). The extent of structural deviation due to the p.D658G variant between the modelled normal and mutated structures of protein was found to have a minimal effect on the protein structure and stability. However, the mutations in the structure of WD40 repeats may hinder the interacting ability of WDR36 with other proteins or may disrupt protein-protein interactions. *In vitro* studies and X-ray crystallography of WDR36 protein are needed to validate the functional effect of the p.D658G variant.

CONCLUSION

It is suggested that the p.D658G mutation is a rare cause of POAG in Punjab region of Pakistan. Overall, the prevalence of mutation p.D658G in the *WDR36* gene is low in our enrolled patients and no variants have been identified in other selected exons. However, mutational frequency may change when a large number of individuals from different regions of Pakistan are screened for this variant. Although the effect of p.D658G on the WDR36 protein structure was explained to be deleterious using *in silico* tools, the exact mechanism and the pathogenicity of this SNP should further be validated by X-Ray crystallography of the WDR36 protein, *in vitro* and *in vivo* experiments and by large population-based studies.

Acknowledgments

We are grateful to all the patients for their participation in this research study. We also appreciate the doctors and staff at the Mughal Eye Hospital, Lahore for their help in recruitment and clinical assessment of the patients.

REFERENCES

Akhtar S., Micheal S., Khan M.I., Yousaf S., Bilal M., Ahmed A. & Qamar R. (2010). Does gender have an effect in the prevalence of types of glaucoma in Pakistani population? *Al-Shifa Journal of Ophthalmology* **6**(1):30–36.

Altschul S.F., Madden T.L., Schaffer A.A., Zhang J., Zhang Z., Miller W. & Lipman D.J. (1997). Gapped BLAST and PSI-BLAST: a new generation of protein database search programs. *Nucleic Acids Research* **25**(17):3389–3402. DOI: https://doi.org/10.1093/nar/25.17.3389

Bui C.M., Chen H., Shyr Y. & Joos K.M. (2005). Discontinuing nasal steroids might lower intraocular pressure in glaucoma. *Journal of Allergy and Clinical Immunology* **116**(5):1042–1047. DOI: https://doi.org/10.1016/j.jaci.2005.07.031

Blaszczyk M., Jamroz M., Kmiecik S., & Kolinski A. (2013). CABS-fold: server for the de novo and consensus-based prediction of protein structure. *Nucleic Acids Researc*h **41**(W1): 406–411. DOI: https://doi.org/10.1093/nar/gkt462

Coutsias E.A., Seok C. & Dill K.A. (2004). Using quaternions to calculate RMSD. *Journal of Computational Chemistry* **25**(15):1849–1857. DOI: https://doi.org/10.1002/jcc.20110

Eswar N., Webb B., Marti-Renom M.A., Madhusudhan M.S., Eramian D., Shen M.Y., Pieper U. & Sali A. (2006). Comparative protein structure modeling using Modeller. *Current Protocols in Bioinformatics* **15**(1): 5–6. DOI: https://doi.org/10.1002/0471250953.bi0506s15

Frezzotti *et al.* (14 authors) (2011). Association between primary open-angle glaucoma (POAG) and WDR36 sequence variance in Italian families affected by POAG. *British Journal of Ophthalmology* **95**(5): 624–626. DOI: https://doi.org/10.1136/bjo.2009.167494

Fuse N. (2010). Genetic bases for glaucoma. *Tohoku Journal of Experimental Medicine* **221**: 1–10. DOI: https://doi.org/10.1620/tjem.221.1

Footz T.K., Johnson J.L., Dubois S, Boivin N., Raymond V. & Walter M.A. (2009). Glaucoma-associated WDR36 variants encode functional defects in a yeast model system. *Human Molecular Genetics* **18**(7): 1276–1287. DOI: https://doi.org/10.1093/hmg/ddp027

Gemenetzi M., Yang Y. & Lotery A.J. (2012). Current concepts on primary open-angle glaucoma genetics: A contribution to disease pathophysiology and future treatment. *Eye* **26**(3):355–369. DOI: https://doi.org/10.1038/eye.2011.309

Guex N. & Peitsch M.C. (1997). SWISS-MODEL and the Swiss-Pdb Viewer: An environment for comparative protein modeling. *Electrophoresis* **18**(15): 2714–2723. DOI: https://doi.org/10.1002/elps.1150181505

Huang X., Li M., Guo X., Li S., Xiao X., Jia X., Liu X. & Zhang Q. (2014). Mutation analysis of seven known glaucoma-associated genes in Chinese patients with glaucoma. *Investigative Ophthalmology and Visual Science* **55**(6): 3594–3602. DOI: https://doi.org/10.1167/iovs.14-13927

Jamroz M. & Kolinski A. (2010). Modeling of loops in proteins: a multi-method approach. *BMC Journal of Structural Biology* **10**(1):1–9. DOI: https://doi.org/10.1186/1472-6807-10-5

Kaur K., Mandal A.K. & Chakrabarti S. (2011). Primary congenital glaucoma and the involvement of CYP1B1. *Middle East African Journal of Ophthalmology* **18**(1): 7–16. DOI: https://doi.org/10.4103/0974-9233.75878

Laskowski R.A., MacArthur M.W., Moss D.S. & Thornton J.M. (1993). PROCHECK: A program to check the stereochemical quality of protein structures. *Journal of Applied Crystallography* **26**(2): 283–291. DOI: https://doi.org/10.1107/S0021889892009944

Mbacham F., Bilong Y., Chedjou, J.P., Nomo A. & Bella A.L. (2020). Variants of WDR36 in Cameroonian glaucoma patients. *Biomedical Science and Engineering* **6**(1): 043–047. DOI: https://doi.org/10.17352/abse.000021

Motushchuk A.E., Komarova T.Y., Grudinina N.A., Rakhmanov V.V., Mandelshtam M.Y., Astakhov Y.S. & Vasilyev V.B. (2009). Genetic variants of CYP1B1 and WDR36 in the patients with primary congenital glaucoma and primary open angle glaucoma from Saint-Petersburg. *Russian Journal of Genetics* **45**(12):1467–1474. DOI: https://doi.org/10.1134/S1022795409120102

Miyazawa A., Fuse N., Mengkegale M., Ryu M., Seimiya M., Wada Y. & Nishida K. (2007). Association between primary open-angle glaucoma and WDR36 DNA sequence variants. *Molecular Vision* **13**: 1912–1919.

Monemi *et al.* (11 authors) (2005). Identification of a novel adult-onset primary open-angle glaucoma (POAG) gene on 5q22. 1. *Human Molecular Genetics* **14**(6): 725–733 DOI: https://doi.org/10.1093/hmg/ddi068

Padgett D.A. & Glaser R. (2003). How stress influences the immune response. *Trends in Immunology* **24**(8): 444–448. DOI: https://doi.org/10.1016/S1471-4906(03)00173-X

Pettersen E.F., Goddard T.D., Huang C.C., Couch G.S., Greenblatt D.M., Meng E.C. & Ferri T.E. (2004). UCSF Chimera: a visualization system for exploratory research and analysis. *Journal of Computational Chemistry* **25**(13): 1605–1612. DOI: https://doi.org/10.1002/jcc.20084

Pasutto F., Mardin C.Y., Michels-Rautenstrauss K., Weber B.H.F., Sticht H., Chavarria-Soley G., Rautenstrauss B., Kruse F. & Resis A. (2008). Profiling of WDR36 missense variants in German patients with glaucoma. *Investigative Ophthalmology and Visual Science* **49**:270–274 DOI: https://doi.org/10.1167/iovs.07-0500

Rezaie T., *et al*. (12 authors) (2002). Adult-onset primary open-

angle glaucoma caused by mutations in optineurin. *Science* **295**(5557): 1077–1079.
DOI: https://doi.org/10.1126/science.1066901

Su H.A., Li S.Y., Yang J.J. & Yen Y.C. (2017). An application of NGS for WDR36 gene in Taiwanese patients with juvenile-onset open-angle glaucoma. *International Journal of Medical Sciences* **14**(12): 1251–1256.
DOI: https://doi.org/10.7150/ijms.20729

Tham Y.C., Li X., Wong T.Y., Quigley H.A., Aung T. & Cheng C.Y. (2014). Global prevalence of glaucoma and projections of glaucoma burden through 2040: a systematic review and meta-analysis. *Ophthalmology* **121**(11): 2081–2090
DOI: https://doi.org/10.1016/j.ophtha.2014.05.013

Van Koolwijk L.M, Despriet D.D., van Duijn C.M., Cortes L.M., Vingerling J.R., Aulchenko Y.S., Oostra B.A., Klaver C.C.W. & Lemij H.G. (2007). Genetic contributions to glaucoma: heritability of intraocular pressure, retinal nerve fiber layer thickness, and optic disc morphology. *Investigative Ophthalmology and Visual Science* **48**(8): 3669–3676.
DOI: https://doi.org/10.1167/iovs.06-1519

Webb B. & Sali A. (2016). Comparative protein structure modeling using MODELLER. *Current Protocols in Bioinformatics* **54**(1): 5–6.
DOI: https://doi.org/10.1002/cpbi.3

Weisschuh N., Wolf C., Wissinger B. & Gramer E. (2007). Variations in the WDR36 gene in German patients with normal tension glaucoma. *Molecular Vision* **13**: 724–729.

Youngblood H., Hauser M.A. & Liu Y. (2019). Update on the genetics of primary open-angle glaucoma. *Experimental Eye Research* **188**: 107795.
DOI: https://doi.org/10.1016/j.exer.2019.107795

Supplementary Table 1: Primer sequences for Exon 8, 11, 13 and 17 of WDR36 gene

Gene	Exon	TM(C')	Forward Primer	Reverse Primer	Product Size
WDR36	8	56°C	ACTGGAGTAAAAGGCAAAGAAA	TCATCTTCTAGGTTGAAAGCTGAT	454bp
	11	55°C	CAGTGGTAATAACATCTTTGTTTTG	TGCTGGTCTTGTGTGAAG ACT	400bp
	13	57°C	GGAATGTTTTAACTTTGGCTTTG	TCTTCTTACACCCCTAAAATC CA	807bp
	17	55°C	GTGGTGACTTTCTGATCAATC	AGCTGTCTACATTATCAAGCAG	443bp